

A Simulation Investigation on the Free Radical Decomposition Mechanism of Hydrogen Peroxide

Xuewu Jia^{a,*}, Fan Zhang^a, Yunxia Xin^b, Wei Xu^a, Ning Shi^a, Zhiguo Lv^b

^aState Key Laboratory of Safety and Control for Chemicals, Research Institute of Safety Engineering, Sinopec, Qingdao 266071, China

^bCollege of Chemical Engineering, Qingdao University of Science and Technology, Qingdao 266042, China
jiaxw.qday@sinopec.com

Hydrogen peroxide (H₂O₂) is an important green inorganic chemical product used widely in pulp bleaching. But H₂O₂ often leads to dangerous explosion accidents in the production and transportation process. In this paper, the Density function theory (DFT) B3LYP method was used to simulate the free radical decomposition mechanism of H₂O₂ at the level of 6-31G(d) basis sets. Geometries of the stationary points were completely optimized. The transition states were validated by the internal reaction coordinate (IRC) calculations. And the reaction energy was found to be -100.65 kJ/mol which is very close to the experimental value.

1. Introduction

Hydrogen peroxide (H₂O₂) is an important green inorganic chemical product, since the final by-products after its application as an oxidant is water and oxygen. It is widely used as oxidant, bleach, disinfectant, deoxidizer, polymerization initiator and a crosslinking agent in various areas of industry, such as chemical synthesis (Biasi et al, 2012), bleaching of pulp, and environment protection (Pintilie et al. 2016).

Valkaj et al. (2015) reported that H₂O₂ was used in the treatment of the Olive oil mill wastewater (OOMW), and the total phenols content diminished by more than 80 % with a 20 % decrease in wastewater's TOC content and leaching below 3 wt. %, which showed a good effect. Ferentz et al. (2016) investigated the mechanism of the phenol treatment by using H₂O₂ and TiO₂ from the view of the structure of the catalyst.

In the recent decades, H₂O₂ is used more and more widely in pulp bleaching (Moral et al. 2016), the production and transportation of which often leads to dangerous explosion accidents (Aberoumand et al. 2016). It is of great significance to study the mechanism of hydrogen peroxide decomposition and to explore the factors that affect the decomposition rate of hydrogen peroxide. According to the reference (Zhang, 2012), the H₂O₂ decomposition mechanism can be implied as follows:



Koussa et al. (2006) has reported the elementary reaction of H₂O₂ reaction with hydrogen atom via the O–O bond destruction path leading to the H₂O molecule and OH radical using the transition state theory (TST). Ab initio (MP2//CASSCF) and density functional theory (B3LYP) methods were used to predict the kinetic parameters, the classical barrier height and the pre-exponential factor.

Hosseini et al. (2013) has reported the effect of methyltrioxorhenium (MTO) for hydrogen peroxide (H₂O₂) decomposition. The thermodynamics of this important system covering the enthalpy and Gibbs energy of the reactions was investigated.

In this paper, the density function theory (DFT) B3LYP (Becke, 1988) and similarly (Lee, 1988) and later (Dickson, 1993) method was used to simulate the free radical decomposition mechanism of H₂O₂ at the level

of 6-31G(d) basis sets. Geometries of the stationary points were completely optimized. The transition states were validated by the internal reaction coordinate (IRC) calculations.

2. Computational method

All the DFT calculations reported in this paper were performed with the Gaussian 03 program (Frisch, 2003) using the B3LYP /6-31 G(d) basis set.

Starting from the transition state geometry, we have performed the IRC calculation of the minimum energy path (MEP) for all the three reactions. The total number of calculated points on the MEP is 95 points in the entrance canal and 54 points in the exit one. The MEP calculation was considered to be converged when a stationary point is reached using a gradient tolerance less than 10^{-5} .

3. Results and discussion

3.1 Electronic structure calculations

In this section, we present our results of the DFT part of calculation relative to the minimum energy structure of each species implied in all three reactions.

The calculated geometrical parameters for the stationary structure of OH \cdot , H₂O, H₂O₂, the reaction complex (RC) and the transition state (TS) (see Figure 1) are given and compared to available experimental ones in Table 1. This table shows that for the calculated parameters of reactants and products agree well with the experimental ones. The relative difference does not exceeds 3 % for bond lengths and 2 % for angles. This difference between calculated and experimental structures verified our calculations and indicates that the resulting moments of inertia of H₂O₂ molecule are predicted with a reasonable accuracy.

Table 1: Calculated geometrical parameters (R, bond lengths in Å; A, bending angle in degree; D, torsional angle in degree)

System	Parameters	DFT calculation	Experiment (Fournier and Depristo, 1992)
H ₂ O ₂	R(O-H)	0.970	0.969
	R(O-O)	1.428	1.464
	A(OOH)	100.5	99.4
	D(HOOH)	113.2	111.8
OH \cdot	R(O-H)	0.979	0.969
H ₂ O	R(O-H)	0.967	0.958
	A(HOH)	104.8	104.5
HOO \cdot	R(O-H)	0.979	
	R(O-O)	1.311	
RC	R(O3-H1)	0.971	
	R(O2-O3)	1.429	
	R(O2-H4)	0.978	
	R(O5-H4)	2.007	
	R(O5-H6)	0.987	
	A(H1O3O2)	100.9727	
	A(O3O2H4)	98.8931	
	A(H4O5H6)	76.275	
TS	D(H1O3O2H4)	116.3687	
	R(O3-H1)	0.973	
	R(O2-O3)	1.399	
	R(O2-H4)	1.053	
	R(O5-H4)	1.347	
	R(O5-H6)	0.978	
	A(H1O3O2)	102.702	
	A(O3O2H4)	102.705	
A(H4O5H6)	101.215		
D(H1O3O2H4)	86.549		

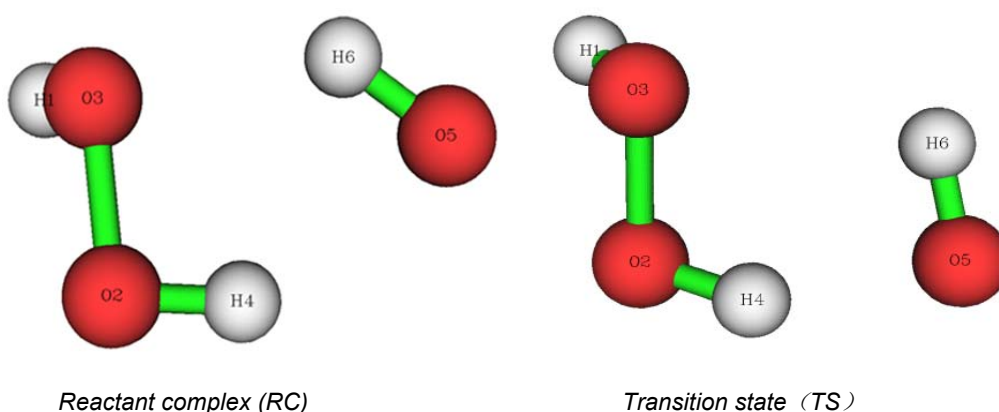


Figure 1: Geometry of the reactant complex (RC) and transition state(TS)

3.2 IRC calculation

3.2.1 Reaction 1

Figure 2 is the potential energy curve of the O-O bond in hydrogen peroxide. It can be seen from the graph that with the increase of the length of the O-O bond, the energy increases gradually, and there is no transition state. For the first step, there is no transition state.

The reaction sites were predicted by analysing the electrostatic potential distribution of H_2O_2 and hydroxyl radical with Multiwfn software as shown in Figure 3. It can be seen that there is a minimum value of electrostatic potential near the oxygen atom in the hydroxyl radical and a maximum value of the electrostatic potential near the H4 atom of H_2O_2 . By the electrostatic action, the O1 in hydroxyl radical would move close to H4 atom, H2 is close to O3, which made the energy decrease to the maximum extent. As a result, the reactant complex (RC) was formed as shown in Figure 1.

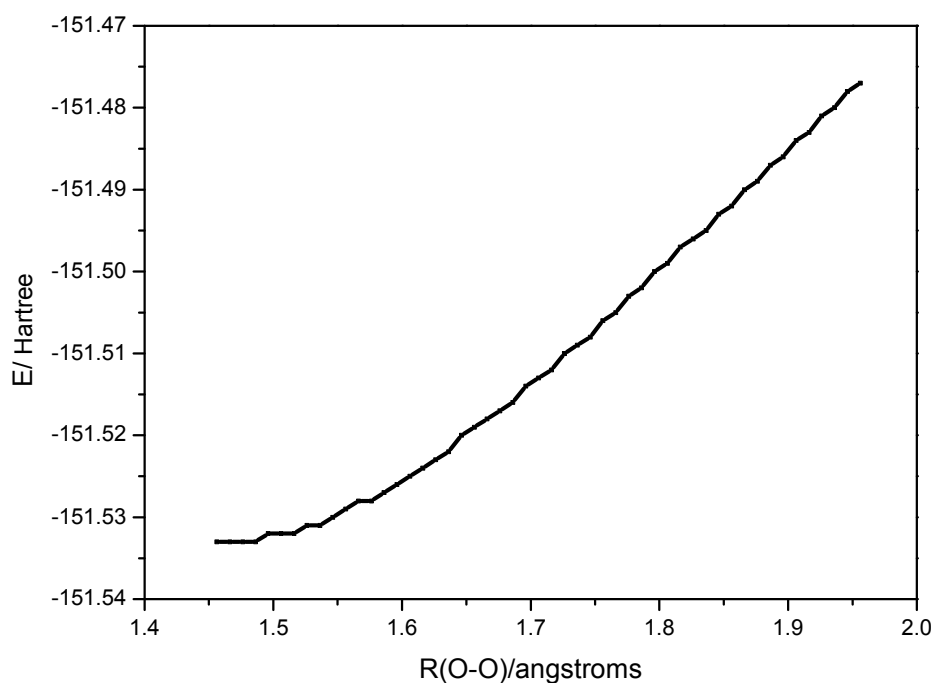


Figure 2: The potential energy curve of broken bond O-O in H_2O_2 .

3.2.2 Reaction 2

Then the dihedral of H_2O_2 decreased from 116.3687 to 86.5487 degrees; the H4 - O2 bond length increased from 0.978 to 1.0532 Å; the O2-O3 bond length shortened from 1.429 to 1.340 Å; the O1 atom of Hydroxyl radical got further close to H4 atom of H_2O_2 , and the transition state (TS) formed. After the O2 - O3 bond was broke and H4 migrated to O5 atom, the products of Reaction 2 were formed.

The frequency of the transition state (TS) was analysed, and there was only one imaginary frequency. The transition states were verified by IRC, and the results showed that the reactants and products were connected by the transition state.

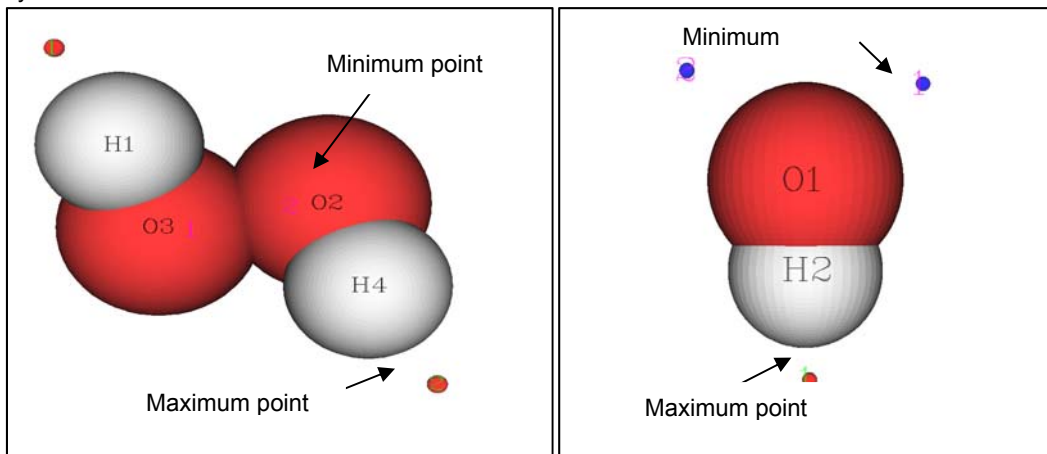


Figure 3: The electrostatic potential distribution of H_2O_2 and hydroxyl radical($\text{OH}\cdot$).

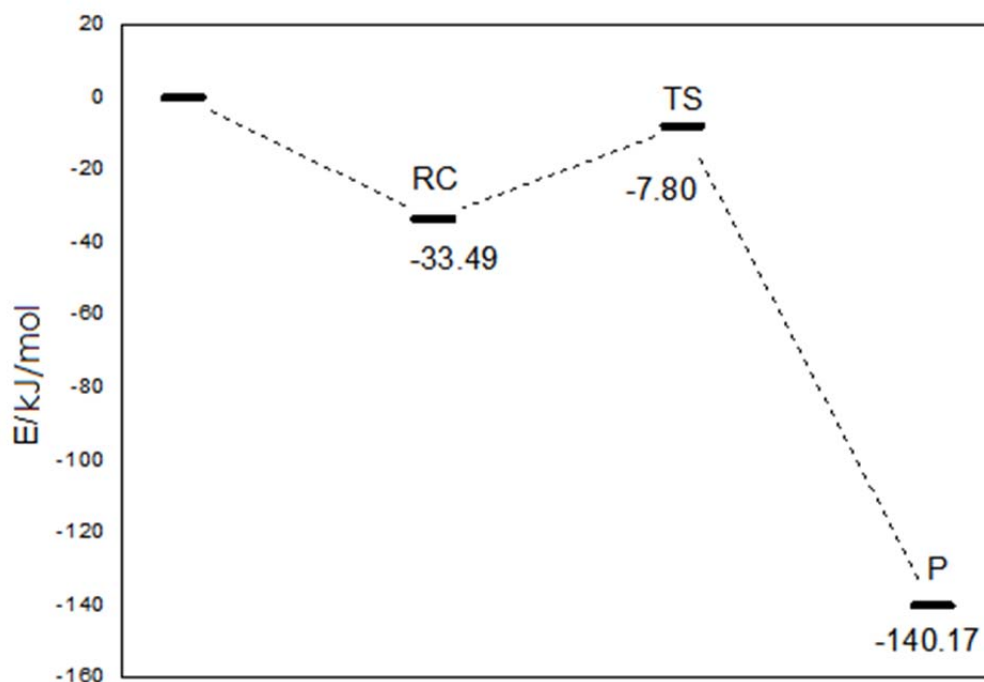


Figure 4: Energy diagrams for the complexes present in Reaction 2.

Figure 4 is the potential energy curve for the Reaction 2 (the total energy of the reactants was set to be zero). As can be seen, the reaction is a single peak reaction. The reaction complex (RC) is 33.49 kJ/mol lower than the reactants. The transition state (TS) energy is slightly higher than that of the reaction complex, and the barrier energy is 26.69 kJ/mol. The reaction is exothermic and the heat released is 140.17 kJ/mol.

3.2.3 Reaction 3

Reaction 3 is the reaction between hydroperoxyl radical (HOO•) and hydroxyl radical (OH•) to produce water and oxygen. Because the basic energy of hydroxyl radical and hydroperoxyl radical is high, it will be converted into product without pass through the transition state.

3.3 Energy analysis

The calculation of the single point energy and the correction of the zero-point energy of each stationary structure s, the reaction complex (RC) and the transition state (TS) in the reaction system was done. The reaction energy is 46.29 kJ/mol of Reaction 1, -140.17 kJ/mol of Reaction 2 and -107.42 kJ/mol of Reaction 3. So, the reaction energy of the total reaction is -100.65 kJ/mol which is very close to the experimental value (-98.4 kJ/mol) (Goor et al. 2007). The transition state (TS) was predicted by analysing the electrostatic potential distribution of H₂O₂ and hydroxyl radical and then simulated to verify it. The reaction mechanism was verified by the IRC calculation.

4. Conclusions

We have performed DFT (B3LYP) calculations using a basis set that is large enough to determine electronic structures of reactants, products and activated complex involved in the decomposition of H₂O₂. The reaction was considered to take place in three steps: the destruction of the O–O bond in H₂O₂, the reaction of H₂O₂ and the hydroxyl radical (OH•), and the formation of H₂O and O₂. The calculated DFT minimum energy structures of the reactant H₂O₂ and the products (OH• and H₂O) were found to be in reasonable agreement with the experimental results. The predicted structure of the transition state (TS) shows that, for Reaction 2 to take place according to the indicated path, the O in hydroxyl radical (OH•) would move close to the H atom of H₂O₂. The transition state (TS) was verified by the IRC calculation. And the reaction energy was found to be -100.65 kJ/mol which is very close to the experimental value. The results of the DFT calculation were useful for the improvement of hydrogen peroxide utilization rate in the pulp industry.

References

- Aberoumand, S., Jafarimoghaddam, A., Moravej, M., Aberoumand, H., Javaherdeh, K., 2016. Experimental study on the rheological behavior of silver-heat transfer oil nanofluid and suggesting two empirical based correlations for thermal conductivity and viscosity of oil based nanofluids, *Applied Thermal Engineering*, 101, 362-372.
- Becke, A. D., 1988. Density-functional exchange-energy approximation with correct asymptotic behaviour, *Physical Review A*, 38(38), 3098-3100.
- Biasi, P., Zancanella, S., Pinna, F., Canu, P., Salmi, T. O., 2011. Hydrogen peroxide direct synthesis: from catalyst preparation to continuous reactors, 24(24), 49-54.
- Dickson, R. M., Becke, A. D., 1993. Basis-set-free local density-functional calculations of geometries of polyatomic molecules. *Journal of Chemical Physics*, 99(5), 3898-3905.
- Ferentz M., Landau M., Vidruk-Nehemya R., Herskowitz M., 2016. Catalytic wet peroxide oxidation of phenol in dark with nanostructured titania catalysts: effect of exposure of anatase 001 plane, *Chemical Engineering Transactions*, 47, 229-234.
- Fournier, R., Depristo, A. E., 1992. Predicted bond energies in peroxides and disulfides by density functional methods, *Journal of Chemical Physics*, 96(2), 1183-1193.
- Frisch, M.J., Trucks, G.W., Schlegel, H.B., Scuseria, G.E., Robb, M.A., Cheeseman, J.R., Montgomery Jr, J.A., Vreven, T., Kudin, K.N., Burant, J.C., Millam, J.M., Iyengar, S.S., Tomasi, J., Barone, V., Mennucci, B., Cossi, M., Scalmani, G., Rega, N., Petersson, G.A., Nakatsuji, H., Hada, M., Ehara, M., Toyota, K., Fukuda, R., Hasegawa, J., Ishida, M., Nakajima, T., Honda, Y., Kitao, O., Nakai, H., Klene, M., Li, X., Knox, J.E., Hratchian, H.P., Cross, J.B., Bakken, V., Adamo, C., Jaramillo, J., Gomperts, R., Stratmann, R.E., Yazyev, O., Austin, A.J., Cammi, R., Pomelli, C., Ochterski, J.W., Ayala, P.Y., Morokuma, K., Voth, G.A.S., Dannenberg, J.J., Zakrzewski, V.G., Dapprich, S., Daniels, A.D., Strain, M.C., Farkas, O., Malick, D.K., Rabuck, A.D., Raghavachari, K., Foresman, J.B., Ortiz, J.V., Cui, Q., Baboul, A.G., Clifford, S., Cioslowski, J., Stefanov, B.B., Liu, G., Liashenko, A., Piskorz, P., Komaromi, I., Martin, R.L., Fox, D.J., Keith, T., Al-Laham, M.A., Peng, C.Y., Nanayakkara, A., Challacombe, M., Gill, P.M.W., Johnson, B., Chen, W., Wong, M.W., Gonzalez, C., Pople, J.A., 2003. GAUSSIAN 03, Revision B03. Gaussian Inc., Pittsburgh.
- Goor, G., Glenneberg, J., Jacobi, S., 2007. Hydrogen Peroxide, in: *Ullmann's encyclopedia of industrial chemistry*. Germany.

- Hosseini, F. N., Nabavizadeh, S. M., Azimi, G., 2013. Theoretical study of the solvent effect on the methyltrioxorhenium/hydrogen peroxide system. *Journal of Solution Chemistry*, 42(11), 2137-2148.
- Koussa, H., Bahri, M., Jaïdane, N., Lakhdar, Z. B., 2006. Kinetic study of the reaction $\text{H}_2\text{O}_2 + \text{H} \rightarrow \text{H}_2\text{O} + \text{OH}$ by ab initio and density functional theory calculations. *Journal of Molecular Structure Theochem*, 770(1), 149-156.
- Lee, C., Yang, W., Parr, R. G., 1988. Development of the colle-salvetti correlation-energy formula into a functional of the electron density. *Phys Rev B Condens Matter*, 37(2), 785.
- Moral, A., Aguado, R., Mutjé, P., Tijero, A., 2016. Papermaking potential of citrus sinensis, trimmings using organosolv pulping, chlorine-free bleaching and refining. *Journal of Cleaner Production*, 112, 980-986.
- Pintilie, L., Torres, C. M., Teodosiu, C., Castells, F., 2016. Urban wastewater reclamation for industrial reuse: an LCA case study. *Journal of Cleaner Production*, 139, 1-14.
- Valkaj, K. M., Kaselj, I., Smolkovic, J., Zrncevic, S., Kumar, N., Murzin, D. Y., 2015. Catalytic wet peroxide oxidation of olive oil mill wastewater over zeolite based catalyst. *Chemical Engineering Transactions*, 43, 853-858.
- Zhang, G. (Ed) 2012. *Hydrogen peroxide production technology*. Beijing, China.